

Evidence for proximity of YFe_2Si_2 to a magnetic quantum critical point

David J. Singh

*Department of Physics and Astronomy, University of Missouri, Columbia, MO 65211-7010, USA**

(Dated: April 30, 2019)

Calculations of the electronic and magnetic properties of the non-magnetic metallic compound YFe_2Si_2 are reported. These show that at the density functional level a magnetic state involving ordering along the c -axis. The electronic structure is three dimensional, and is similar to that of the unconventional superconductor YFe_2Ge_2 and as well as that of the high pressure collapsed tetragonal phase of KFe_2As_2 , which is also a superconductor. Based on the results in relation to experiment, we infer that properties of YFe_2Si_2 are strongly influenced by a nearby antiferromagnetic quantum critical point.

I. INTRODUCTION

There is renewed interest in metals with unusual magnetic behavior. This is due in part to the unusual magnetic properties of the Fe-based superconductors, [1–5] and spin-fluctuation pairing models for these and other unconventional superconductors. [6–12] Within such models superconductivity depends both on the details of the spin-fluctuations, particularly their strength and momentum dependence, and the electronic structure, i.e. the Fermi surface and the coupling of states on it with the spin fluctuations. In Fe-based superconductors, the electronic structure involves several d orbitals, hybridized with ligand p -states, and formed by both hopping through ligand orbitals and direct Fe-Fe hopping. In most cases, this leads to disconnected hole and electron sheets of Fermi surface connected by antiferromagnetic fluctuations associated with a stripe magnetic order. [10, 11, 13] However, there are heavily electron doped materials, such as $\text{K}_x\text{Fe}_2\text{Se}_2$, that apparently only have electron Fermi surfaces, but are still high temperature superconductors. [14–18] This both presents a challenge for theory and suggests exploration for other compounds that might show different forms of Fe-based superconductivity.

While Fe-based superconductivity has generally been restricted to pnictides and chalcogenides, Zou, Chen and co-workers, [19, 20] have recently reported superconductivity in the germanide, YFe_2Ge_2 with $T_c=1.8$ K. There is strong evidence both from experiment [19, 20] and theory [21, 22] that the superconductivity is unconventional, but the symmetry of the superconducting state has not been established. In any case, this first finding of Fe-based superconductivity in a compound with a group IV ligand suggests exploration of chemically related compounds. Here we report investigation of the silicide, YFe_2Si_2 .

YFe_2Si_2 is an Fe-based compound that occurs in the ThCr_2Si_2 structure, [23] is metallic and does not show ordered magnetism in experiment. However, while there is no magnetic ordering, there a significant variation in the reported magnetic properties perhaps due to sample

differences. [24–32]

II. METHODS AND STRUCTURE

The present density functional theory (DFT) calculations were done using the generalized gradient approximation of Perdew, Burke and Ernzerhof (PBE) [33] and the linearized augmented planewave (LAPW) method [34] as implemented in the WIEN2k code. [35] LAPW sphere radii of 2.4 bohr, 2.4 bohr and 1.85 bohr were used for Y, Fe and Si respectively. Well converged basis sets consisting of local orbitals for the upper core states of Y and Fe and LAPW functions up to a cutoff determined by $R_{\text{Si}}k_{\text{max}}=7$, corresponding to an effective $R_{\text{Fe}}k_{\text{max}} \simeq 9$ for the metal atoms, were used. The calculations were based on the experimental lattice parameters, $a=3.92$ Å, $c=9.92$ Å. [23] The internal coordinate, corresponding to the Si height above the Fe plane, was determined by energy minimization as discussed below.

As mentioned, the internal coordinate of Si in the unit cell was determined by energy minimization. Within our density functional calculations we find a magnetic ground state in contrast to experiment. We did the relaxation both for a non-spin-polarized case and for ferromagnetic order. With ferromagnetic order we obtain a Si position, $z_{\text{Si}}=0.3710$, as compared to 0.3673 without spin polarization. Thus including ferromagnetic order increases the Fe-Si distance from 2.280 Å to 2.298 Å. Unless, noted otherwise the results presented below are based on the ferromagnetic Si position. Magnetism is predicted in the DFT calculations independent of this choice of Si position. We note that there is a similar but larger effect of magnetism on the structure, particularly the ligand height, in the Fe-based superconductors. This includes compositions that are not magnetically ordered in experiment. In the Fe-based superconductors the best agreement with the experimental structure is obtained from magnetic calculations. [4]

* singhdj@missouri.edu

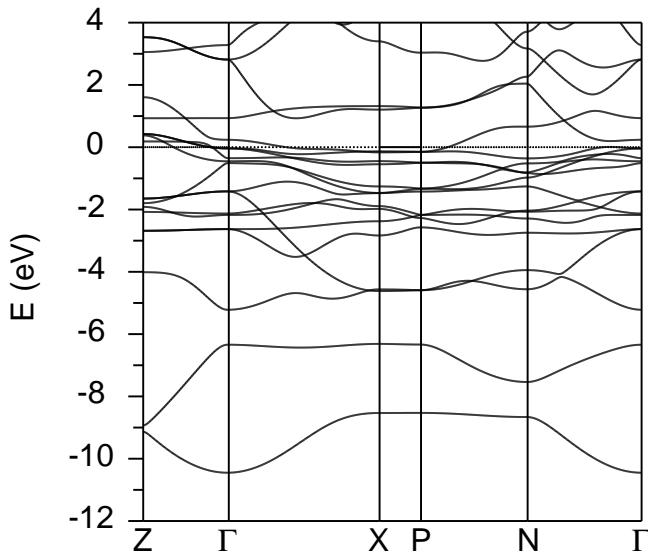


FIG. 1. Calculated non-spin-polarized band structure of YFe_2Si_2 .

III. RESULTS

We start by discussing the electronic structure as obtained without spin-polarization. The calculated band structure is shown in Fig. 1, with the corresponding electronic density of states and projection of Fe d character in Fig. 2. The lowest two bands in Fig. 1, (~ -11 eV $-$ -6 eV), are from the Si s orbitals, while the higher valence bands shown are derived from Si p and Fe d orbitals. The bands from -3 eV to 2 eV (relative to the Fermi energy, E_F) have predominant Fe character, hybridized with Si. Y occurs as Y^{3+} , with the Y $4d$ states located entirely above E_F as may be expected. The orbital characters of the Fe d bands around E_F are shown in the fat band plots of Fig. 3.

As seen, there are five bands crossing the Fermi level. The resulting five Fermi surfaces are depicted in Fig. 4. These involve multiple d orbitals. The density of states at the Fermi level is $N(E_F)=5.47$ eV^{-1} per formula unit (two Fe atoms). The corresponding bare specific heat coefficient is $\gamma_{bare}=12.9$ mJ/mol K^2 . It will be interesting to compare this with experiment to determine the specific heat renormalization, which is $\gamma/\gamma_{bare} \sim 10$ in the germanide superconductor, YFe_2Ge_2 . [20] Since $N(E_F)$ comes from d bands, the Stoner criterion for itinerant magnetism [36, 37] is clearly exceeded, and so the non-spin-polarized state is unstable against magnetism at the DFT level.

The calculated plasma frequencies are $\Omega_{p,xx}=\Omega_{p,yy}=3.33$ eV and $\Omega_{p,zz}=4.59$ eV. Based on this, YFe_2Si_2 is an anisotropic three dimensional metal. This means that from an electronic point of view the material is well connected along the c -axis direction. This reflects Si-Si bonding, analogous to the Ge-Ge bonding that has been discussed in YFe_2Ge_2 , [20–22]

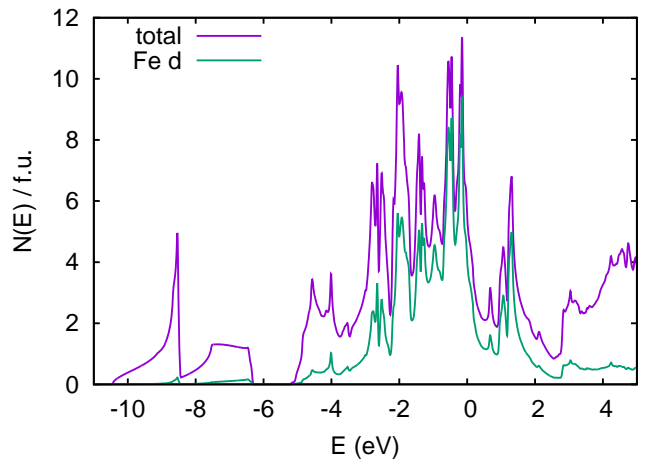


FIG. 2. Calculated electronic density of states and Fe d projection on a per formula unit basis (note that there are two Fe atoms per formula unit).

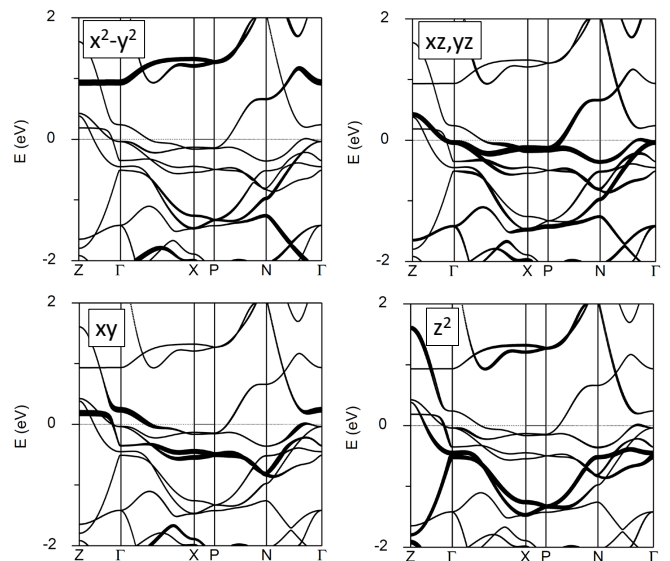


FIG. 3. Bands near the Fermi energy, emphasizing different Fe d orbital characters by fat bands. The coordinate systems for the orbital character is the square lattice defined by the Fe plane, which is rotated 45° from the tetragonal a and b lattice directions for the two Fe atom unit cell.

and As-As bonding the collapsed tetragonal phase of KFe_2As_2 . [20] Assuming that the scattering is relatively k -independent, this would imply a high conductivity direction along c , with an anisotropy $\sigma_c/\sigma_a \sim 1.9$. However, as discussed below, the calculations suggest strong spin fluctuations coupled to parts of the Fermi surface, which may produce different scattering on different sheets and a temperature dependent anisotropy, reflecting the evolution of the spin fluctuations with temperature.

As mentioned, there are five bands crossing E_F . These lead to five sheets of Fermi surface, consisting of four

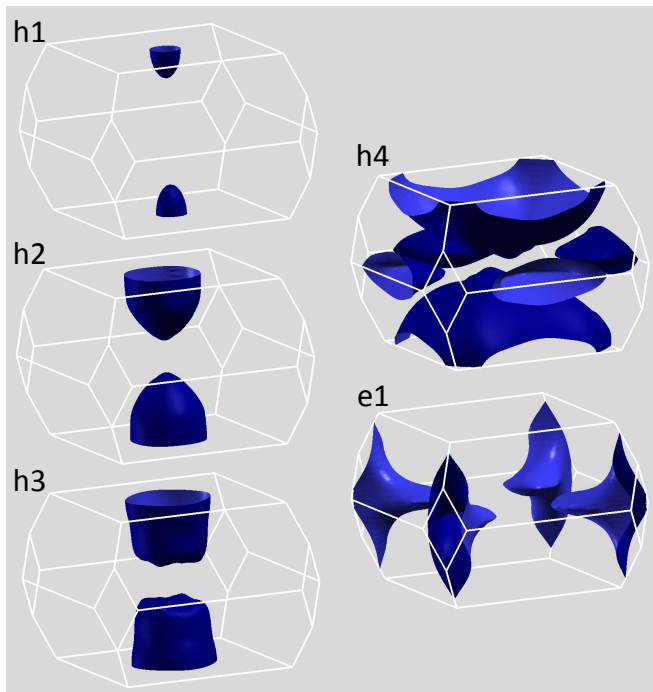


FIG. 4. Fermi surfaces of YFe_2Si_2 , showing four hole sheets (h1,h2,h3,h4) and one electron sheet (e1).

closed hole sections, and an open corrugated cylindrical electron section along the zone corners, as depicted in Fig. 4. The electron count in YFe_2Si_2 is odd, so the electron and hole sections are not compensated, and the hole sections are dominant. The hole sheets consist of four closed sections, h1, h2, h3, and h4, centered at the Z point, and containing 0.008, 0.107, 0.154 and 0.893 holes per formula unit, respectively. The electron cylinder at the zone corner (e1) contains 0.161 electrons per formula unit. The orbital character of the small h1 section is z^2 (here we use the coordinate system of the Fe-square plane, which is rotated 45° with respect to the a and b axes of the two Fe atom unit cell), while the other three hole sections have mixed character involving all the d orbitals except $x^2 - y^2$. The electron cylinder has predominantly xz, yz and xy character.

As anticipated from the value of $N(E_F)$, which exceeds the Stoner criterion, magnetism is expected at the DFT level. We do find a ferromagnetic instability, as expected. The calculated spin magnetization is $1.39 \mu_B$ per two Fe atom unit cell. This comes from a spin moment of $0.75 \mu_B$ per Fe (as measured by the magnetization in the Fe LAPW sphere, radius 2.4 bohr) partly compensated by a back polarization on Si. This is, however, not the calculated ground state.

We did calculations for several different possible orderings, as summarized in Table I. These were ferromagnetic (F), C-type order (C), which is a checkerboard antiferromagnetism in the Fe plane, with like spin Fe stacked on top of each other to make ferromagnetic chains in the c -axis direction, G-type order (G), which is checker-

TABLE I. Calculated energies and total density of states, $N(E_F)$ for different magnetic configurations, on a per formula unit (two Fe) basis, with energies relative to the non-spin-polarized (NSP) state.

	E (eV/f.u.)	$N(E_F)$ (eV^{-1})
NSP	0	5.45
F	-0.033	5.84
C	-	-
G	-	-
A	-0.050	4.08
A4	-0.045	4.89
S1	-0.026	4.40
S2	-0.030	4.29
S3	-0.035	4.40
X	-	-
XZ	-0.011	4.87

board in plane stacked antiferromagnetically in the c direction, and A-type order (A), which is ferromagnetic F planes stacked antiferromagnetically. We also did calculations for a double period A type order (A4), consisting of double ferromagnetic Fe layers, stacked antiferromagnetically (...UUDDUDD... along c), stripe type chain order in the Fe-planes, as in the Fe-pnictide superconductors, stacked ferromagnetically along c , (S1), stacked to run at 90° in alternating planes (S2), and stacked antiferromagnetically along c (S3). Finally, we consider a double stripe order, which in plane is an X -point order (ferromagnetic Fe chains running diagonally with respect to the Fe square lattice), stacked ferromagnetically along c (X) and antiferromagnetically along c (XZ). Stable solutions were not found for G, C or X order, and instead imposing these ordering patterns amounted to the non-spin-polarized state.

The results (Table I) show that energy differences between different ordering patterns and the energy difference between the non-spin-polarized state and the ground state are comparable, and some orders do not have solutions at all. This is a signature of itinerant magnetism, in the sense that there are not stable atomic moments that exist independent of the ordering.

The lowest energy orderings are the A-type and A4-type, with the A-type lower. The lowest energy A-type order also gives the lowest $N(E_F)$, which might suggest a role for electrons at the Fermi energy in stabilizing it. However, examining the other states, there is no clear trend between $N(E_F)$ and energy among the other antiferromagnetic orderings.

The energies show antiferromagnetic stackings along c are favored, but that this is not representable in terms of a single c -axis exchange constant. For example, the energy difference between the A-type and ferromagnetic orders, which differ flipping every c -direction bond from ferromagnetic to antiferromagnetic is ~ 27 meV/formula unit, while for the stripe order (S1 - S3) this difference

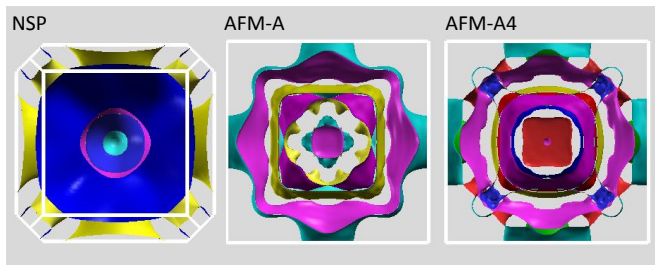


FIG. 5. c -axis view of the Fermi surface for the non-spin-polarized case, and the A-type and A4 (see text) orders.

is only 9 meV/formula unit. Finally, and most remarkably, while the $F - A$ energy difference suggests a high energy cost for making ferromagnetic stacking, the A4 structure, which has ferromagnetic sheets with half the c -direction bonds ferromagnetic and half antiferromagnetic has an energy only 5 meV per formula unit above the ground state. The energies therefore suggest an important role for band structure and itinerant electrons in the magnetism.

Returning to the band structure, a two fold degenerate heavy band and a single degenerate band cross E_F at almost the same point along the Γ - Z line. These three bands correspond to the h2,h3 and h4 Fermi surfaces. The crossing is at ~ 0.19 of the Γ - Z distance. Noting the flattened end of the h3 surface and the flattened disk shape of h4, there is an implied nesting at a distance of $\sim 0.37 \times 2\pi/c$. This is intermediate between the periodicity of the A and A4 magnetic structures (0.5 and 0.25, respectively). Fig. 5 shows a view along k_z of the Fermi surfaces for the A and A4 magnetic states in comparison with that of the NSP calculation. As seen, these magnetic orders gap away the large parts of these hole sections, in particular producing new reconstructed cylindrical sections from the large hole pancake (h4). This suggests that spin fluctuations associated with this order would affect transport in the c -axis direction more strongly than in the plane, leading to a disproportionate reduction in conductivity along c and a temperature dependent conductivity anisotropy.

This provides an explanation for the stability of these two magnetic structures. It also resolves an experimental puzzle regarding the magnetic structure of the rare earth substituted compounds. In particular, neutron diffraction experiments on NdFe_2Si_2 found Nd moments ordered with a ferromagnetic in plane order and a c -axis ...UDDUU... order, which was not readily understood in terms of reasonable superexchange pictures. [38] However, Fermi surface nesting similar to what we find, along with a slight shift in the nesting vector closer to 0.25 could readily explain this pattern.

Fig. 6 shows the density of states, comparing the NSP calculations with the lowest energy A-type antiferromagnetic case and the stripe ordered S3 case. As seen, the density of states is reconstructed over the energy range of the Fe d bands, i.e. -3 eV to 2 eV, on going from the

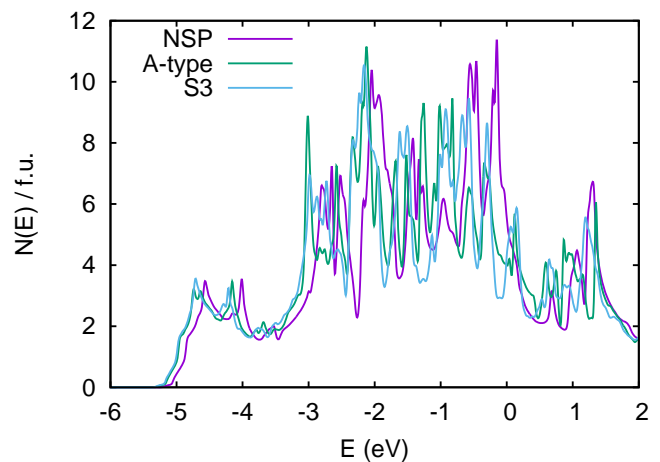


FIG. 6. Density of states for non-spin-polarized, the ground state A-type antiferromagnetic state, and the S3 state.

NSP state to either of the antiferromagnetic states plotted. This is a characteristic of transition metal magnets and reflects the coupling of the d orbitals. It is the basis of the Stoner theory, which assumes rigid shifts of the d bands on forming ferromagnetic moments. [36, 37, 39, 40] It is a feature of both local moment and itinerant transition metal magnets, and is seen for example in the itinerant antiferromagnet Cr. [41] Importantly, comparing the A-type and S3 densities of states, it is clear that they similarly differ over the range of the d bands. This is a signature of the importance of band structure effects in the magnetism, including both bands near E_F and bands at energies away from the Fermi level. This is similar to the Fe-based superconductors. [42]

Thus, at the DFT level, YFe_2Si_2 is a magnetic compound, with a ground state having ferromagnetic layers, stacked antiferromagnetically, and with a substantial itinerant character. The magnetic order couples strongly to sections of the Fermi surface, particularly the largest hole sheets. The related A4 structure is close in energy, and these compete with a strip magnetic order analogous to that of the Fe-based superconductors. In plane checkerboard antiferromagnetism is strongly disfavored. Experimentally, on the other hand no magnetic order is reported. This discrepancy is similar to YFe_2Ge_2 , [21, 22, 43] which is an unconventional superconductor and appears to be near a magnetic quantum critical point (note that LuFe_2Ge_2 is magnetically ordered). [19, 44]

The situation for YFe_2Si_2 is less clear, perhaps in part because of sample differences. Mössbauer experiments for the iso-structural $R\text{Fe}_2\text{Si}_2$ compounds (R =rare earth), indicated the Fe has no moment in these compounds. However, broadenings were seen in the ^{57}Fe spectra. These were interpreted as originating in induced Fe moments from the rare earth site. [24, 25] Detailed studies show smooth variations in lattice parameters and Mössbauer spectra across the series, similar to the $R\text{Fe}_2\text{Ge}_2$ compounds. [24–26] The R =La,Y,Lu

compounds, where there are no rare earth moments, are reported to be ordinary Pauli paramagnetic metals. [24, 27, 28] On the other hand, magnetic behavior is readily induced by Cr alloying, [28] and there are reports that show evidence for multiple Fe sites, with magnetic behavior on a portion of the Fe perhaps associated with Fe-Si disorder. [29, 30] Other unusual magnetic behavior has also been reported under pressure and with doping. [31, 32] In any case, it is clear that experiment does not show behavior consistent with the A-type magnetic order predicted in DFT calculations.

IV. DISCUSSION AND CONCLUSIONS

The electronic structure of metallic YFe_2Si_2 is found to be very similar to YFe_2Ge_2 , including the qualitative structure of the Fermi surface and the band character. Importantly, DFT calculations predict an antiferromagnetic A-type ground state, competing with stripe order. This is in contrast to experiment, which shows Pauli paramagnetism. This type of discrepancy in which standard DFT calculations overestimate the tendency towards magnetism is unusual. More commonly DFT cal-

culations underestimate the tendency towards moment formation as is the case in several classes of strongly correlated materials, including cuprates. Overestimation of the tendency to magnetism in DFT calculations is however a characteristic of the Fe-based superconductors. [4] It is found as well in metals near quantum critical points associated with itinerant magnetism. In that case the discrepancy is a consequence of renormalization by spin-fluctuations associated with the critical point and not included in standard DFT calculations. [45–47]

The behavior found for YFe_2Si_2 is similar to that found for YFe_2Ge_2 , except that (1) the magnetic energy scale is lower in the silicide and (2) the ordering of the magnetic states more strongly favors the A type ordering relative to ferromagnetism or the stripe orders. It will be of interest to attempt synthesis of high quality well ordered crystals of YFe_2Si_2 in order to measure its physical properties in detail, especially specific heat and transport to assess the extent to which magnetic fluctuations influence its properties. In addition, spectroscopic experiments on Fe-based superconductors and YFe_2Ge_2 have shown evidence of quantum spin fluctuations in splittings of the Fe 3s core level under ambient conditions. [5, 43] Similar experiments for YFe_2Si_2 would be of interest.

-
- [1] D. C. Johnston, *Adv. Phys.* **59**, 803 (2010).
 [2] G. R. Stewart, *Rev. Mod. Phys.* **83**, 1589 (2011).
 [3] M. D. Lumsden and A. D. Christianson, *J. Phys. Condens. Matter* **22**, 203203 (2010).
 [4] I. I. Mazin, M. D. Johannes, L. Boeri, K. Koepernik, and D. J. Singh, *Phys. Rev. B* **78**, 085104 (2008).
 [5] F. Bondino, E. Magnano, M. Malvestuto, F. Parmigiani, M. A. McGuire, A. S. Sefat, B. C. Sales, R. Jin, D. Mandrus, E. W. Plummer, D. J. Singh, and N. Mannella, *Phys. Rev. Lett.* **101**, 267001 (2008).
 [6] D. J. Scalapino, E. Loh, and J. E. Hirsch, *Phys. Rev. B* **34**, 8190 (1986).
 [7] N. D. Mathur, F. M. Grosche, S. R. Julian, I. R. Walker, D. M. Freye, R. K. W. Haselwimmer, and G. G. Lonzarich, *Nature* **394**, 39 (1998).
 [8] M. D. Johannes, I. I. Mazin, D. J. Singh, and D. A. Papaconstantopoulos, *Phys. Rev. Lett.* **93**, 097005 (2004).
 [9] T. Moriya, *Proc. Jpn. Acad. B* **82**, 1 (2006).
 [10] I. I. Mazin, D. J. Singh, M. D. Johannes, and M. H. Du, *Phys. Rev. Lett.* **101**, 057003 (2008).
 [11] K. Kuroki, S. Onari, R. Arita, H. Usui, Y. Tanaka, H. Kontani, and H. Aoki, *Phys. Rev. Lett.* **101**, 087004 (2008).
 [12] D. J. Scalapino, *Rev. Mod. Phys.* **84**, 1383 (2012).
 [13] D. J. Singh and M. H. Du, *Phys. Rev. Lett.* **100**, 237003 (2008).
 [14] J. Guo, S. Jin, G. Wang, S. Wang, K. Zhu, T. Zhou, M. He, and X. Chen, *Phys. Rev. B* **82**, 180520 (2010).
 [15] M. H. Fang, H. D. Wang, C. H. Dong, Z. J. Li, C. M. Feng, and H. Q. Yuan, *Europhys. Lett.* **94**, 27009 (2011).
 [16] L. Zhang and D. J. Singh, *Phys. Rev. B* **79**, 094528 (2009).
 [17] T. Qian, X. P. Wang, W. C. Jin, P. Zhang, P. Richard, G. Xu, X. Dai, Z. Fang, J. G. Guo, X. L. Chen, and H. Ding, *Phys. Rev. Lett.* **106**, 187001 (2011).
 [18] Z. R. Ye, Y. Zhang, F. Chen, M. Xu, J. Jiang, X. H. Niu, C. H. P. Wen, L. Y. Xing, X. C. Wang, C. Q. Jin, B. P. Xie, and D. L. Feng, *Phys. Rev. X* **4**, 031041 (2014).
 [19] Y. Zou, Z. Feng, P. W. Logg, J. Chen, G. Lampronti, and F. M. Grosche, *Phys. Stat. Sol. Rapid Res. Lett.* **8**, 928 (2014).
 [20] J. Chen, K. Semeniuk, Z. Feng, P. Reiss, P. Brown, Y. Zou, P. W. Logg, G. I. Lampronti, and F. M. Grosche, *Phys. Rev. Lett.* **116**, 127001 (2016).
 [21] A. Subedi, *Phys. Rev. B* **89**, 024504 (2014).
 [22] D. J. Singh, *Phys. Rev. B* **89**, 024505 (2014).
 [23] D. Rossi, R. Marazza, and R. Ferro, *J. Less Common Met.* **58**, 203 (1978).
 [24] A. M. Umarji, D. R. Noakes, P. J. Viccaro, G. K. Shenoy, A. T. Aldred, and D. Niarchos, *J. Magn. Magn. Mater.* **36**, 61 (1983).
 [25] D. R. Noakes, A. M. Umarji, and G. K. Shenoy, *J. Magn. Magn. Mater.* **39**, 309 (1983).
 [26] J. J. Bara, H. U. Hryniewicz, A. Milos, and A. Szytula, *J. Less Common Metals* **161**, 185 (1990).
 [27] A. Dommann, F. Hulliger, and C. Baerlocher, *J. Less Common Metals* **138**, 113 (1988).
 [28] I. Ijjaali, G. Venturini, and B. Malaman, *J. Alloys Compds.* **279**, 102 (1998).
 [29] S. G. Sankar, S. K. Malik, V. U. S. Rao, and R. Obermeyer, *API Conf. Proc.* **34**, 236 (1976).
 [30] I. Felner, I. Mayer, A. Grill, and M. Schieber, *Solid State Commun.* **16**, 1005 (1975).
 [31] I. Felner, B. Lv, K. Zhao, and C. W. Chu, *J. Supercond. Nov. Magn.* **28**, 1207 (2015).
 [32] I. Felner, B. Lv, and C. W. Chu, *J. Phys. Condens.*

- Matter **25**, 476002 (2014).
- [33] J. P. Perdew, K. Burke, and M. Ernzerhof, Phys. Rev. Lett. **77**, 3865 (1996).
- [34] D. J. Singh and L. Nordstrom, *Planewaves Pseudopotentials and the LAPW Method, 2nd Edition* (Springer, Berlin, 2006).
- [35] P. Blaha, K. Schwarz, G. Madsen, D. Kvasnicka, and J. Luitz, *WIEN2k, An Augmented Plane Wave + Local Orbitals Program for Calculating Crystal Properties* (K. Schwarz, Tech. Univ. Wien, Austria, 2001).
- [36] E. C. Stoner, Proc. R. Soc. London Ser. A **169**, 339 (1939).
- [37] J. F. Janak, Phys. Rev. B **16**, 255 (1977).
- [38] H. Pinto and H. Shaked, Phys. Rev. B **7**, 3261 (1973).
- [39] O. K. Andersen, J. Madsen, U. K. Poulsen, O. Jepsen, and J. Kollar, Physica B **86-88**, 249 (1977).
- [40] G. L. Krasko, Phys. Rev. B **36**, 8565 (1987).
- [41] H. L. Skriver, J. Phys. F **11**, 97 (1981).
- [42] M. D. Johannes and I. I. Mazin, Phys. Rev. B **79**, 220510 (2009).
- [43] N. Sirica, F. Bondino, S. Nappini, I. Pis, L. Poudel, A. D. Christianson, D. Mandrus, D. J. Singh, and N. Mannella, Phys. Rev. B **91**, 121102 (2015).
- [44] T. Fujiwara, N. Aso, H. Yamamoto, M. Hedo, Y. Saiga, M. Nishi, Y. Uwatoko, and K. Hirota, J. Phys. Soc. Jpn. **76**, SA60 (2007).
- [45] T. Moriya, *Spin Fluctuations in Itinerant Electron Magnetism* (Springer, Berlin, 1985).
- [46] I. I. Mazin and D. J. Singh, Phys. Rev. B **69**, 020402 (2004).
- [47] M. Shimizu, Rep. Prog. Phys. **44**, 329 (1981).